International Journal of Modern Physics A

THE NEAR–THRESHOLD PRODUCTION OF ϕ–MESONS IN PROTON–NUCLEON COLLISIONS

M .Hartmann[1,*], Y. Maeda[1,2,†], I. Keshelashvili[1,3], S. Barsov[4], W. Borgs[1], M. Büscher[1], V.I. Dimitrov[5], S. Dymov[6], A. Dzyuba[1,4], V. Hejny[1], A. Kacharava[3,7], V. Kleber[8], H.R. Koch[1], V. Koptev[4], P. Kulessa[1,9], T. Mersmann[10], S. Merzliakov[7], S. Mikirtytchiants[4], A. Mussgiller[1,5], M. Nekipelov[1], M. Nioradze[3], H. Ohm[1], K. Pysz[9], R. Schleichert[1], H.J. Stein[1], H. Ströher[1], Yu. Valdau[4], K.–H. Watzlawik[1], C. Wilkin[11] and P. Wüstner[12] for the ANKE collaboration

[1] *Institut für Kernphysik, Forschungszentrum Jülich, 52425 Jülich, Germany*
[2] *Institut für Kernphysik, Universität zu Köln, 50937 Köln, Germany*
[3] *High Energy Physics Institute, Tbilisi State University, 0186 Tbilisi, Georgia*
[4] *High Energy Physics Department, Petersburg Nuclear Physics Institute, 188350 Gatchina, Russia*
[5] *Idaho Accelerator Center, Pocatello, Idaho 83209, USA*
[6] *Laboratory of Nuclear Problems, Joint Institute for Nuclear Research, 141980 Dubna, Russia*
[7] *Physikalisches Institut II, Universität Erlangen–Nürnberg, 91058 Erlangen, Germany*
[8] *Physikalisches Institut, Universität Bonn, 53115 Bonn, Germany*
[9] *H. Niewodniczański Institute of Nuclear Physics PAN, 31342 Kraków, Poland*
[10] *Institut für Kernphysik, Universität Münster, 48149 Münster, Germany*
[11] *Physics and Astronomy Department, UCL, Gower Street, London WC1E 6BT, UK*
[12] *Zentralinstitut für Elektronik, Forschungszentrum Jülich, 52425 Jülich, Germany*

Received Day Month Year
Revised Day Month Year

The $pp \to pp\phi$ and quasi–free $pn \to d\phi$ reactions have been studied at the Cooler Synchrotron COSY–Jülich, using the internal beam and the ANKE facility. Total cross sections in the pp entrance channel have been determined at three excess energies ϵ in the range of $18.5-75.9$ MeV. In case of the pn entrance channel the energy dependence of the cross section up to 80 MeV has been extracted by exploiting the intrinsic momentum of the neutron inside a deuterium target. Taken together with data for ω–production, a significant enhancement of the ϕ/ω ratio for both entrance channels of a factor 8 is found compared to predictions based on the Okubo–Zweig–Iizuka rule.

Keywords: ϕ–meson; Meson production; OZI rule.

PACS numbers: 25.40.Ve, 13.75.Cs

*E-mail address: M.Hartmann@FZ-Juelich.de
†Present address: Research Center for Nuclear Physics, Osaka University, Ibaraki, Osaka 567–0047, Japan

1. Introduction

Meson production has the potential to clarify important questions of hadron physics in the non–perturbative regime of QCD. The production of the non-strange pseudoscalar mesons $\pi(140)$, $\eta(547)$, and $\eta'(958)$ has been systematically studied in proton–proton and partially in proton–neutron interactions (see *e.g.* Ref. [1]), whereas for the vector mesons the data base is comparatively sparse. The $\phi(1020)$–meson is of particular interest because of its large mass, corresponding to a distance of two colliding nucleons $\approx 0.2\,\mathrm{fm}$, and its dominant $s\bar{s}$ quark content.

The relative production rates of the isoscalar ω (consisting mainly of $u\bar{u}$ and $d\bar{d}$) and ϕ mesons is interesting in view of the so–called Okubo–Zweig–Iizuka (OZI) rule [2]. This ratio may shed light on the strange-quark admixture in the nucleon [3], if the production mechanisms are understood and similar in both cases [4,5,6]. Precise data in the near–threshold region are required since here only the lowest partial waves contribute, which simplifies the theoretical interpretation of the data.

Total ω–production cross sections have been measured in proton–proton collisions for excess energies ϵ from a few MeV up to several GeV [7,8,9,10]. On the other hand, data for $pp\phi$ are very scarce; total cross sections have been obtained for $\epsilon \sim (2-4)\,\mathrm{GeV}$ [11,12], while at low excess energy a single measurement of total and differential cross sections has been made by the DISTO collaboration at $\epsilon = 83\,\mathrm{MeV}$ [9].

Lipkin predicted a ϕ–to–ω production ratio of $R_{\phi/\omega} = 4.2 \times 10^{-3} \equiv R_{\mathrm{OZI}}$ [13,14]. The DISTO ϕ data, in combination with the ω cross section of COSY-TOF at $\epsilon = 92\,\mathrm{MeV}$ [8], yield an enhanced value of $R_{\phi/\omega} \sim 7 \times R_{\mathrm{OZI}}$. The differential distributions from DISTO indicate that ϕ production proceeds dominantly via the ${}^3P_1(pp)$ entrance channel, though contributions of higher partial waves have also been seen. To clarify this, it is crucial to extend the measurements to such small excess energies that only the lowest partial waves can contribute. Such measurements have become feasible at the internal proton beam of the Cooler Synchrotron COSY at the Research Centre Jülich, using the ANKE target and detector facility described in Sect. 2.

In order to study all facets of meson production dynamics, it is necessary to investigate the isospin dependence by precision measurements in both pp as well as pn collisions. In the case of the η–meson, such experiments have revealed that the pn production cross section is over six times larger than that for pp [15]. Analogous ϕ data are important for nucleon–nucleon production models and also serve as crucial input in the interpretation of nucleon-nucleus, and nucleus-nucleus results, where *in–medium* effects are anticipated [16].

In Sect. 3 the ANKE results for ϕ production in proton–proton collisions at three beam momenta, corresponding to excess energies of $\epsilon = 18.5$, 34.5 and 75.9 MeV, are summarized [17]. In Sect. 4 the results on the quasi–free $pn \to d\phi$ reaction in the energy range up to 80 MeV are presented [18]. Our conclusions are to be found in Sect. 5.

2. Experimental set–up

The measurements were carried out at the ANKE magnetic spectrometer [19] situated at the internal beam of COSY. ANKE comprises three dipole magnets D1–D2, which guide the circulating beam through a variable chicane (see Fig. 1). Charged particles resulting from beam–target interactions are deflected by the central dipole D2 (1.6 T) onto the ANKE detector systems, on the left (right) side of the beam for negatively (positively) charged particles. The cluster–jet target can be operated with hydrogen (areal density $\sim 5\times10^{14}\,\mathrm{cm}^{-2}$) and deuterium ($\sim 3.4\times10^{14}\,\mathrm{cm}^{-2}$) gas [20].

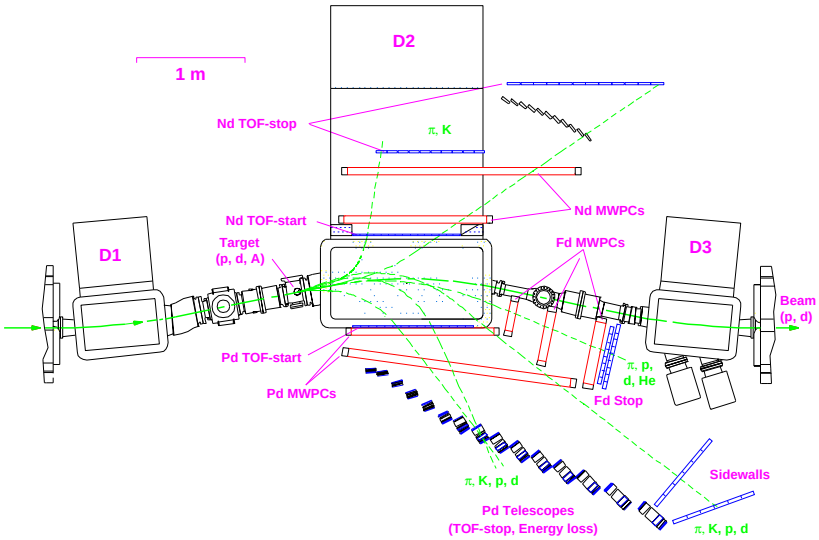

Fig. 1. Schematic representation of the ANKE spectrometer.

Both the $pp\to pp\phi$ and $pn\to d\phi$ reactions have been studied by detecting the K^+K^- decay of the ϕ mesons in coincidence, respectively, with one of the forward–going protons or with the forward–going deuteron. The overall missing masses in both channels were required to be consistent with the non–observed second proton in the first case, and the non–observed slow spectator proton, *i.e.* $pd\to d\phi\, p_{\mathrm{sp}}$, in the second.

In the first step of the data analysis, positive kaons are selected through a procedure described in detail in Ref. [21], using the time of flight (TOF) between START and STOP scintillation counters of a dedicated K^+ detection system. The forward–going protons or deuterons are identified from the time–of–flight differences between the STOP counters in the forward detector systems with respect to the K^+ STOP counter. Figure 2 shows, for the deuterium target, the absolute time difference between protons/deuterons and the K^+ TDC values versus the time difference reconstructed via the measured momenta of both particles.

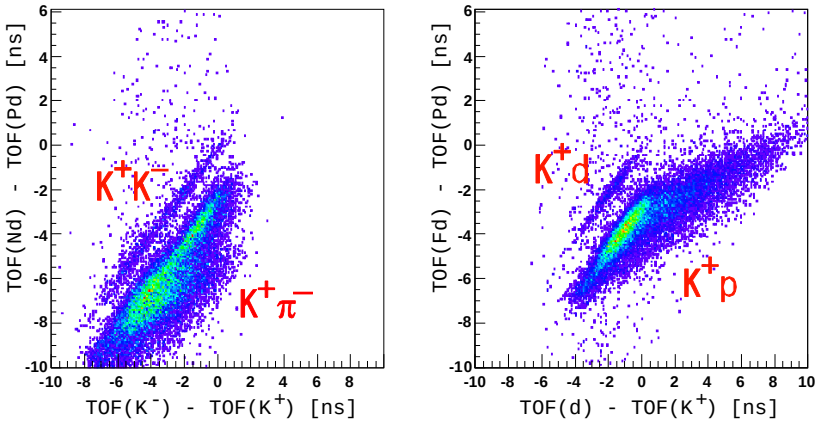

Fig. 2. Absolute time difference between negative (lhs) or forward (rhs) STOP counters relative to the positive STOP counter in comparison with the time differences reconstructed from the particle momenta.

2.1. *Detection System for Negatively Charged Ejectiles at ANKE*

The ANKE experiments COSY–104 and COSY–147 (see Ref. [28]) require the detection of K^- mesons and for this a new detector system was constructed [29] supplementing the existing detectors for positively charged particles [19]. It is placed partly inside the return yoke of the C–shaped D2 dipole magnet (stray field up to $\approx 200\,\mathrm{mT}$). At the maximum field of D2 (1.6 T), negatively charged ejectiles can be measured in the momentum range from 120 to 1000 MeV/c. The horizontal and vertical angular acceptances are (roughly): $\alpha_{\mathrm{hor}} = \pm 12°$; $\alpha_{\mathrm{ver}} = \pm 8°$ at 120 MeV/c and $\alpha_{\mathrm{hor}} = -2°$ to $12°$, $\alpha_{\mathrm{ver}} = \pm 5°$ at 1 GeV/c. Negatively charged pions can also be detected in this system so that, taken in combination with the positive detection systems, many additional reactions on elementary and nuclear targets can be investigated at ANKE.

For time of flight (TOF) measurements, the system contains 2 mm thin START and 10 mm and 20 mm thick STOP scintillator counters for the low and high momentum region respectively. The measured time resolution between the START and STOP counters is insufficient to distinguish between π^- and K^- with momenta above 500 MeV/c. To obtain a better particle separation — in particular for measurements on nuclear targets where the missing–mass technique generally cannot be used — dedicated curved Čerenkov counters have been installed in front of the high momentum STOP counters. Two multi-wire proportional chambers — identical to those on the positive side — are placed between the START and STOP counters for particle–momentum reconstruction.

Figure 2 shows the absolute time differences between the assumed kaon particles. A clear separation of K^+K^- correlations from the $K^+\pi^-$ background is possible on the basis of such plots.

3. The $pp \to pp\phi$ reaction

To obtain total cross sections of ϕ-meson production, the average luminosity was determined through the simultaneous measurement of pp elastic scattering. At the lowest excess energy of ϵ=18.5 MeV this was cross–checked with an alternative method which determines the target density by measuring the frequency shift of the circulating proton beam due to its energy loss during the repeated passages through the target. Using the known beam current the luminosity can thus be determined [22].

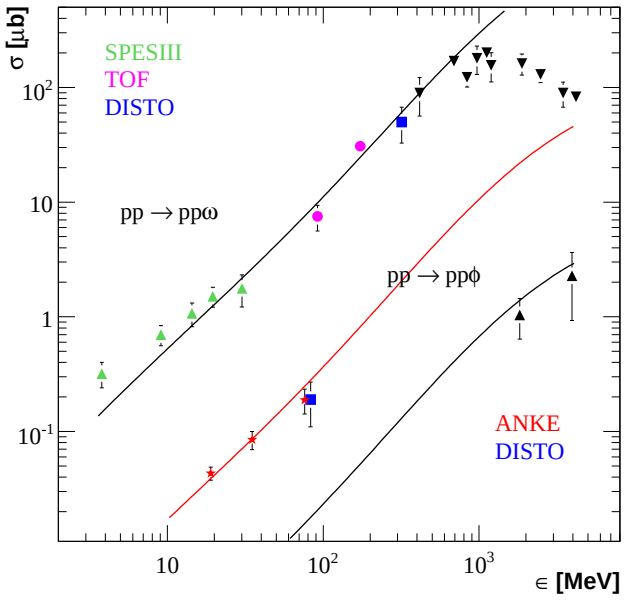

Fig. 3. Total ϕ– and ω–production cross sections in pp collisions. The three lines show the energy dependence of three–body phase space including the effect of final–state–interaction (FSI) normalized to the ω (top) and ϕ (middle and bottom) cross sections. The middle line is normalized to the three low–energy ANKE points (stars), while the lowest line is fixed by the high energy ϕ cross sections.

Figure 3 shows the ANKE ϕ-production cross sections at ϵ = 18.5 MeV, 34.5 MeV, and 75.9 MeV [17] together with DISTO result [9] and the data at high energies [11,12]. The results for ω production are also indicated [7,8,10]. The three lines show the energy dependence of three–body phase space including the effect of pp final–state interaction (FSI), see Ref. [23]. The line in the middle is normalized to the three ANKE cross sections (stars) at low energies and clearly fails to describe the high energy ϕ data. For comparison the lowest line is fixed to pass through the high energy data. The ϕ/ω production ratio thus changes from $\sim (1-2.4) \times R_{\rm OZI}$ at the high energies to $\sim 8 \times R_{\rm OZI}$ in the near–threshold region.

The differential distributions at ϵ=18.5 MeV demonstrate the dominance of the transition from the $^3P_1$ (pp) entrance channel to the $^1S_0(pp)$ final state together with

a clear effect of proton–proton FSI (see Ref. [17]). Whereas at $\epsilon = 83\,\mathrm{MeV}$ DISTO also observed the dominance of the ${}^3P_1 \to {}^1S_0$ transition [9], they did not see any indication of the pp FSI in their proton momentum spectrum, and this is essentially consistent with our findings at $\epsilon = 75.9\,\mathrm{MeV}$. Figure 4 shows the dependence of the ANKE cross section at $\epsilon = 75.9\,\mathrm{MeV}$ on the pp relative momentum (light crosses) in comparison with a phase–space calculation (solid line). The DISTO distribution at slightly higher energy is also included. Taking both results together, it is tempting to

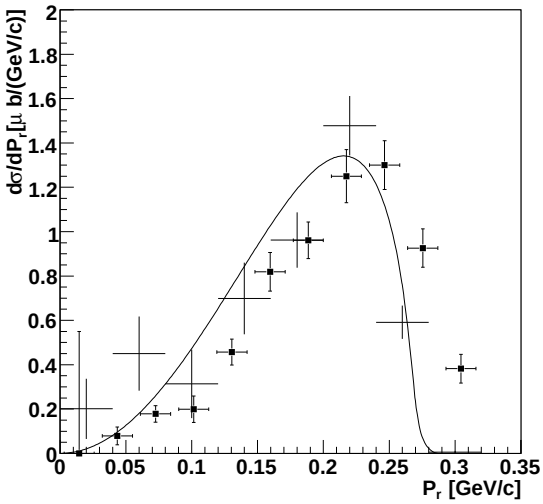

Fig. 4. Dependence of the cross section (light crosses) on the pp relative momentum at $\epsilon = 75.9\,\mathrm{MeV}$. The solid line reflects pure phase space. The black squares are the DISTO data at $\epsilon = 83\,\mathrm{MeV}$.

ask what mechanisms might obscure the effect of final–state interactions at moderate excess energies. There could be contributions from higher partial waves, but more exotic explanations, such as the existence of a ϕN–resonance (see Ref. [23]), have also been advocated.

4. The quasi–free $pn \to d\phi$ reaction

In order to select quasi–free $pn \to d\phi$ production from the measured $pd \to d\phi\, p_{\mathrm{sp}}$ reaction, the missing mass of the (K^+, K^-, deuteron) candidates has been calculated and a gate put around the proton mass. The momentum distribution of the unobserved proton for the events in the ϕ mass region shows the expected distribution for a spectator (details are given in Ref. [18]). The luminosity was derived from measurements of the effective target thickness and the beam current.

Figure 5 shows the energy dependence of the quasi–free $pn \to d\phi$ production together with the total cross sections obtained from $pp \to pp\phi$ [17]. Though the $pn \to d\phi$

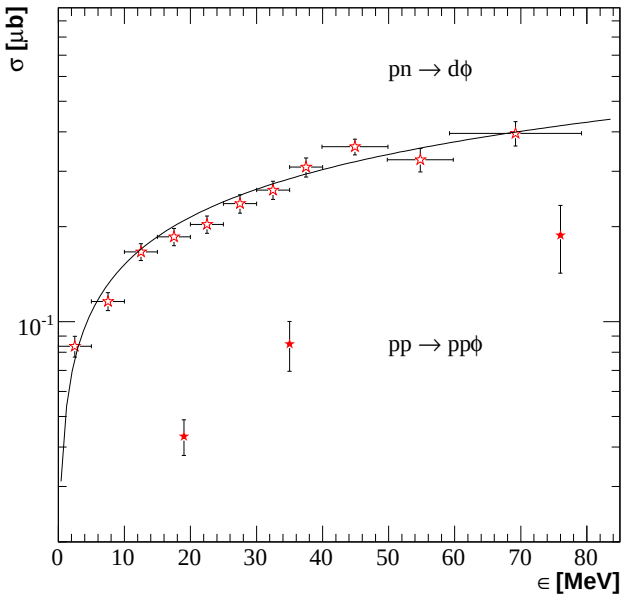

Fig. 5. Total cross section for the quasi–free $pn \to d\phi$ reaction as a function of the excess energy (error bars indicate the statistical uncertainties). The curve represents a phase–space $\sqrt{\epsilon}$ calculation. For comparison, the values obtained for $pp \to pp\phi$ are also included.

cross sections are consistent with a phase–space $\sqrt{\epsilon}$ behavior the kaon angular distributions show the presence of p waves at rather low energy [18].

Very close to threshold, isoscalar s–wave ϕpn production can be estimated from the $d\phi$ data using FSI theory [24] and this approach yields a ratio $\sigma(pn \to pn\phi)/\sigma(pp \to pp\phi) \approx 2.3 \pm 0.5$. Compared with η production [15], the ratio is about three times smaller.

5. Conclusion and Outlook

As already noted the ϕ– to ω–production ratio in pp collisions is enhanced in the near–threshold region. With the existing $pn \to d\omega$ data measured at 57^{+21}_{-15} MeV[25], the production ratio at this energy is found to be $\sigma(pn \to d\phi)/\sigma(pn \to d\omega) = (4.0 \pm 1.9) \times 10^{-2} \approx 9 \times R_{\mathrm{OZI}}$. This value is similar to that found in the pp case, though the error bar is here much larger.

The combined results of ϕ–meson production in pp and pn collisions at ANKE allows one to resume theoretical works on the understanding of strangeness production. The enhanced ϕ/ω–production ratio in the near–threshold region may be a signal for additional dynamical effects related to the role of strangeness in few nucleon systems. For a more detailed discussion of the ANKE results in the pp and pn entrance channels we refer to Refs. [17,18].

To clarify the partial wave contributions in pp collisions a new ANKE measurement has been performed and the number of detected ϕ mesons at $\epsilon = 75.9\,\mathrm{MeV}$

was increased from ≈ 200 up to several thousands (see Ref. [28]). The analysis is in progress and the data will be also used to study a possible compact ϕp system [23,26].

Acknowledgments

Support from J. Haidenbauer, C. Hanhart, U.–G. Meißner, A. Sibirtsev, Yu. Uzikov, K. Nakayama, and other members of the ANKE Collaboration [27], as well as the COSY machine crew, are gratefully acknowledged. This work has been partially financed by the BMBF, DFG, Russian Academy of Sciences, and COSY FFE.

References

1. C. Hanhart, Phys. Rep. **397**, (2004) 155.
2. S. Okubo, Phys. Lett. **5** (1963) 165; G. Zweig, CERN report TH-**401** (1964); J. Iizuka, Prog. Theor. Phys. Suppl. **38** (1966) 21.
3. J. Ellis *et al.*, Phys. Lett. B **353** (1995) 319; Nucl. Phys. A **673** (2000) 256.
4. K. Tsushima and K. Nakayama, Phys. Rev. C **68** (2003) 034612.
5. A. Faessler *et al.*, Phys. Rev. C **70** (2004) 035211.
6. L.P. Kaptari and B. Kämpfer, Eur. Phys. J. A **23** (2005) 291.
7. F. Hibou *et al.*, Phys. Rev. Lett. **83** (1999) 492.
8. S. Abd El-Samad *et al.*, Phys. Lett. B **522** (2001) 16.
9. F. Balestra *et al.*, Phys. Rev. C **63** (2001) 024004.
10. A. Baldini *et al.*, in *Numerical Data and Functional Relationships in Science and Technology, Total Cross–Sections for Reactions of High Energy Particles*, edited by H. Schopper, Landolt–Börnstein, New Series, Group **1**, Vol. **12** (Springer–Verlag, Berlin, Heidelberg, 1998).
11. R. Baldi *et al.*, Phys. Lett. B **68** (1977) 381.
12. V. Blobel *et al.*, Phys. Lett. B **59** (1975) 88.
13. H.J. Lipkin, Phys. Lett. B **60** (1976) 371; current data lead to $R_{\rm OZI} = 3.53 \times 10^{-3}$, see Ref. [14].
14. S. Eidelmann *et al.*, Phys. Lett. B **592** (2004) 1.
15. H. Calén *et al.*, Phys. Rev. Lett. **80** (1998) 2069; H. Calén *et al.*, Phys. Rev. C **58** (1998) 2667.
16. G.E. Brown and M. Rho, Phys. Rep. **269** (1996) 333.
17. M. Hartmann *et al.*, Phys. Rev. Lett. **96** (2006) 242301.
18. Y. Maeda *et al.*, Phys. Rev. Lett. (*to be published*); nucl-ex/0607001.
19. S. Barsov *et al.*, Nucl. Instr. Meth. A **462** (2001) 364.
20. A. Khoukaz *et al.*, Eur. Phys. J. D **5** (1999) 275.
21. M. Büscher *et al.*, Nucl. Instr. Meth. A **481** (2002) 378.
22. K. Zapfe, Nucl. Instrum. Meth. A **368** (1996) 293.
23. A. Sibirtsev, J. Haidenbauer, and U.–G. Meißner, Eur. Phys. J. A **27** (2006) 263.
24. G. Fäldt and C. Wilkin, Phys. Lett. B **382** (1996) 209.
25. S. Barsov *et al.*, Eur. Phys. J. A **21** (2004) 521.
26. M. Hartmann *et al.*, Nucl. Phys. A **755** (2004) 459.
27. The ANKE Collaboration: http://www.fz-juelich.de/ikp/anke.
28. M. Hartmann *et al.*, COSY Proposal: No. **104** and No. **147**, http://www.fz-juelich.de /ikp/publications/List_of_all_COSY-Proposals.shtml.
29. H.R. Koch, annual report FZ-Jülich (1999) p. 28;
M. Hartmann *et al.*, annual report FZ-Jülich (2002): http://www.fz-juelich.de /ikp/publications/AR2002/de/chap01.shtml#1 (see 8. and 9.).